

Interaction Notes

Note 629

1 June 2019

Modeling of Cable Conduits with Nonlinear Permeability

Dr. F.M. Tesche

 Consultant (Retired)

Dr. D. V. Giri

Pro-Tech and Dept. of ECE, University of New Mexico, Albuquerque, NM

Giri@DVGiri.com www.dvgiri.com

and

Dr. Armin Kälin

Formerly with armasuisse, now with EMProtec, Switzerland

Abstract

This note discusses an electrical model for estimating the effects of magnetic field saturation in a ferromagnetic conduit, or shield. Starting with Maxwell's equations, a diffusion equation describing the magnetic field within the conduit material is developed. While this diffusion equation cannot be solved analytically for the general nonlinear case, due to the dependence of the permeability on the ambient magnetic field amplitude, may be solved numerically using a finite difference time domain (FDTD) method. The steps in performing this analysis are described and several sample results are illustrated. The representation of the nonlinear behavior of the magnetic permeability of the conduit material is important in conducting such an analysis. A relatively simple functional form for the material magnetization curve is suggested and used in the sample analysis.

In this note, a sample calculation is performed for the iron conduit, which has been discussed in previous reports. An earlier analysis suggested that a linear relative permeability of $\mu_r = 200$ is appropriate for this material. Using this value, a hypothetical nonlinear magnetization curve is developed and a calculation of the per-unit-length excitation voltage of shielded wires within the conduit is conducted. Additional calculations for this cable conduit will require a more accurate determination of the material magnetization properties.

1. Introduction

In previous reports detailing the effects of a direct lightning strike to a building with a buried cable conduit, a transfer impedance model was used to estimate the excitation of signal wires within the protective conduit [1], [2]. A portion of the direct lightning strike to the building can flow along the conduit, and due to the resistance of the conduit, there is a voltage drop along the conduit. This voltage excites the wires inside the conduit and the resulting current flow may cause problems in the equipment connected to the end of the cables.

For non-magnetic conduit materials, such as aluminum or copper, the transfer impedance model is straightforward due to the inherent linearity in the electrical properties of the material. However, for the case of the iron tube, it is recognized that the permeability (μ) of the material is usually a nonlinear function of the magnetic field intensity (H). This implies that the shielding provided by the iron tube and other magnetic type conductors is not easily described by the linear transfer impedance concept discussed in [1].

The study of electromagnetic shielding by materials with nonlinear permeability is not a new subject. An early report on electromagnetic pulse (EMP) shielding and relationships to the physical properties of the material (iron in this case) was described by Young [3]. Later, Merewether investigated the EMP shielding effects of a planar magnetic shield [4]. He subsequently extended this analysis to cylindrical cable shields [5], much like the geometry under consideration in the present paper. Karzas and Mo [6] investigated EMP diffusion through a ferromagnetic conducting slab, and developed a number of relationships to describe the complicated shielding behavior of such a nonlinear material. Croisant, et. al. [7] and [8] have discussed the conduit shielding problem for a ferromagnetic magnetic material, and have introduced in the concept of effective permeabilities, from which the peak value and the time constant of the internal electric field may be estimated.

This note reviews the development of a procedure for computing the shielding of a magnetic tubular shield, or conduit. In this discussion, we will define a diffusion equation for the magnetic field penetrating into the conduit material and indicate how the internal E-field can be calculated. A numerical example for the results of this calculation will be provided. Key in conducting this solution is the representation of the magnetization (B-H) curve of the ferromagnetic material. A simple representation of this property is suggested.

2. Calculation of the Conduit Shielding for Ferromagnetic Materials

The geometry of the problem under consideration is illustrated in Figure 1. The protective conduit surrounding the internal signal wire (or wires) is constructed of magnetic material having conductivity σ and nonlinear permeability $\mu(H)$. The permeability is not considered to be a function of frequency in the frequency regime that is relevant in this note. This conduit has inner and outer radii of a and b , respectively.

The external lightning induced current on the conduit is denoted as I_s and it creates an external magnetic field H_ϕ^{ext} as illustrated in the figure. The magnetic field can diffuse through the imperfectly conducting shield and this results in a longitudinal electric field E_z on the inner surface of the conduit. We first find the magnetic field that diffuses through and then get the axial electric field through Maxwell's curl equation. It is this field that provides the excitation of the inner conductor. Determining this field is the goal of this study.

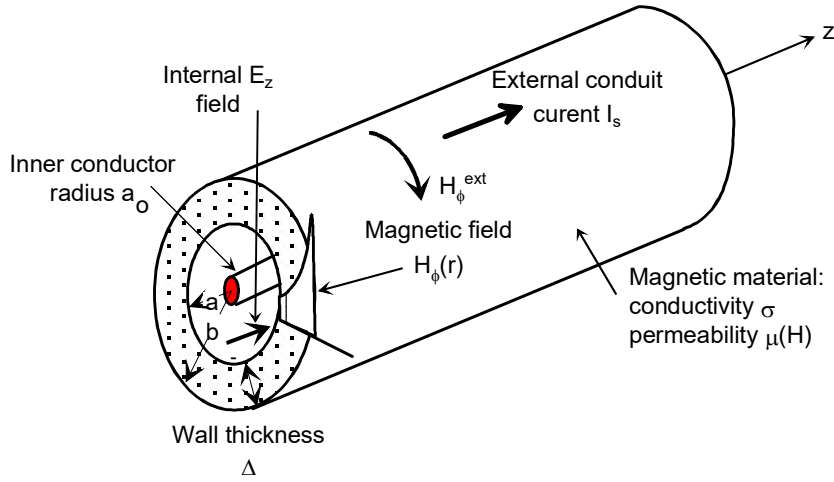


Figure 1. Illustration of the problem geometry.

2.1 Description of the Penetrating Magnetic Field

In the previous work for shielding by magnetic materials, the solution for the internal electromagnetic (em) fields is obtained by a numerical solution of Maxwell's equations. In the linear case, such a solution may be obtained analytically. However, for the case of a nonlinear magnetic material this is not possible.

The starting point for this analysis is Maxwell's equations for the E and H field within the conduit material:

$$\nabla \times \vec{H} = \frac{\partial \vec{D}}{\partial t} + \sigma \vec{E} \quad (1a)$$

$$\nabla \times \vec{E} = -\frac{\partial \vec{B}}{\partial t} \quad (1b)$$

Neglecting the displacement current $\partial\vec{D}/\partial t$ in the shield material when compared with the conduction current σE , taking the curl of Eq.(1a), and substituting into Eq.(1b), results in the vector diffusion equation for the magnetic field

$$\nabla \times \nabla \times \vec{H} = -\sigma \frac{\partial \vec{B}}{\partial t}. \quad (2)$$

Using the chain rule, the temporal derivative can be expressed as

$$\frac{\partial \vec{B}}{\partial t} = \left(\frac{\partial B}{\partial H} \right) \frac{\partial \vec{H}}{\partial t} \equiv \mu(H) \frac{\partial \vec{H}}{\partial t} \quad (3)$$

where the nonlinear permeability $\mu(H) = \partial B / \partial H$ is defined to be the *slope* of the B-H magnetization curve of the nonlinear magnetic material. As a result, the expression for the internal H-field in the conduit material becomes

$$\nabla \times \nabla \times \vec{H} = -\sigma \mu(H) \frac{\partial \vec{H}}{\partial t}. \quad (4)$$

For the cylindrical geometry assumed in Figure 1, only the H_ϕ field component exists. Furthermore, we assume there is no ϕ or z variation of these fields. In this case, the expression for the H-field simplifies to

$$\frac{1}{r} \frac{\partial}{\partial r} \left(r \frac{\partial H_\phi}{\partial r} \right) - \frac{H_\phi}{r^2} - \sigma \mu(H) \frac{\partial H_\phi}{\partial t} = 0. \quad (5)$$

Equation (5) is valid for $H_\phi(r;t)$ inside the conduit material for $a \leq r \leq b$ and for time $t \geq 0$. The solution for $H_\phi(r;t)$ must obey the initial condition $H_\phi(r;0) = 0$ and boundary conditions at $r = a$ and b , which require $H_\phi(a;t) = 0$ and $H_\phi(b;t) = H_\phi^{ext}(t)$, where $H_\phi^{ext}(t)$ is the external tangential H-field on the surface of the conduit resulting from the induced lightning current. The boundary condition $H_\phi(a;t) = 0$ is an approximation in the sense the permeability is sufficiently high, and we do satisfy this condition in our analysis, as shown later following Eq.(15). The difference (b-a) is the wall thickness Δ . In such material shielding problems, it has been found that the typical time constant of the diffused field is orders of magnitude longer than the time constant of the excitation field [9]. Thus, for times scales appropriate for describing the *internal* H-fields, the *external* field can be approximated by an impulse function as

$$H_\phi^{ext}(t) \approx q_o \delta(t), \quad (6)$$

where the impulse of the field q_o represents the area under the transient H-field curve. This quantity has the units of (A/m)-s, or Coul/m, and represents the charge density on the circumference of the wire that is carried by the current I_s . This can be expressed in terms of the total charge carried by the conduit current as

$$H_\phi^{ext}(t) \approx \frac{Q_o}{2\pi b} \delta(t), \quad (7)$$

where

$$Q_o = \int_0^{\infty} I_s(t) dt . \quad (8)$$

2.2 Description of the Penetrating Electric Field

Once the internal H-field is determined from a solution to Eq.(5), the corresponding E-field can be evaluated by using Eq.(1a) as

$$\vec{E} = \frac{1}{\sigma} \nabla \times \vec{H} . \quad (9)$$

Specializing this expression to the H_ϕ field component existing for this problem yields the expression

$$E_z(r) = \frac{1}{\sigma} \frac{1}{r} \frac{\partial}{\partial r} (r H_\phi) . \quad (10)$$

Of special importance is this E-field at the inner surface $r = a$, as it forms the per-unit-length voltage excitation source for the internal wires.

2.3 Evaluation of the Penetrating EM Fields

As mentioned earlier, the solution to the nonlinear diffusion equation for the H-field in Eq.(5) cannot be obtained analytically for a general nonlinear permeability $\mu(H)$. It is possible, however, to obtain a solution using to a finite difference time domain (FDTD) approximation to this equation [10]. In doing this, the variable r is divided into $(n+1)$ equally spaced points over the range $[a,b]$, in the space between the inner and outer conductor, with the distance between each point denoted by Δ_r . For the variable i running from 0 to $n+1$, these spatial points are denoted as r_i , with $r_0 = a$ and $r_{n+1} = b$. At each location, the H-field is denoted as H_i , where the subscript ϕ has been dropped for convenience.

At a particular point i , the first order spatial derivative for the H-field is approximated as

$$\left. \frac{\partial H}{\partial r} \right|_{r_i} \approx \frac{H_{i+1} - H_i}{\Delta_r} . \quad (11)$$

The second order derivative is

$$\left. \frac{\partial^2 H}{\partial r^2} \right|_{r_i} \approx \frac{H_{i+1} + H_{i-1} - 2H_i}{\Delta_r^2} . \quad (12)$$

Using a forward time difference for the temporal derivative as

$$\frac{\partial H(t)}{\partial t} \approx \frac{H_i(t + \Delta_t) - H_i(t)}{\Delta_t} = \frac{H_i^{new} - H_i}{\Delta_t} , \quad (13)$$

where H_i^{new} denotes an updated value of the H-field and Δ_t is the time step, Eq.(5) can be cast into a series of equations for updating the H-fields at the discrete locations r_i :

$$H_i^{new} = H_i + \frac{\Delta_t}{\sigma \mu(H_i)} \left[\left(\frac{1}{\Delta_r^2} + \frac{1}{r\Delta_r} \right) H_{i+1} + \frac{1}{\Delta_r} H_{i-1} - \left(\frac{2}{\Delta_r^2} + \frac{1}{r\Delta_r} + \frac{1}{r^2} \right) H_i \right] \quad (14)$$

for the index $i = 1$ to n . Notice that the values of H_0 and H_{n+1} are fixed by the boundary conditions at $r = a$ and $r = b$, and they are not updated. H_0 is zero at $r = a$ as a starting point.

The solution for the transient H-field within the conduit material is achieved by marching Eq.(14) along in time and evaluating H_i^{new} at all locations using the results of the fields from a previous time step. At each time step and at each location, the appropriate magnetic permeability $\mu(H_i)$ must be evaluated. Estimates of this function are provided in Section 3. This process is critically dependent on the choice of the time step Δ_t , which is usually determined by trial and error. Using a time step that is too large will cause the simulation to become unstable. However, too small a time step will result in very long computation times. The optimum value of this time step is strongly dependent on the character of the nonlinearity in the function $\mu(H)$.

Once the solution for the H-fields in the mesh is completed, the discrete version of Eq.(10) can be used to find the E_z -field at $r = a$. This is expressed as

$$\begin{aligned} E_z &\approx \frac{1}{\sigma} \frac{1}{r_0} \frac{(r_1 H_1 - r_0 H_0)}{\Delta_r} = \frac{1}{\sigma} \frac{(a + \Delta_r)}{a \Delta_r} H_1 \\ &\approx \frac{1}{\sigma \Delta_r} H_1 \end{aligned} \quad (15)$$

The last part of the Eq. (15) is valid because $\Delta_r \ll a$. We also note that H_0 is zero and thus the boundary condition at $r = a$ is also satisfied.

2.4 Model Development and Validation

A computer program has been developed based on the forgoing theory to compute the tangential E_z field on the interior of the conduit. This code assumes that the excitation current I_s is a unit impulse function, so that the value of Q_0 in Eq.(8) is unity. As a check of the operation of this program, it is useful to compare its results for a known case — namely for the iron conduit considered previously in ref.[1]. For this shield, the following parameters were assumed:

- Inner radius $a = 41.25$ mm
- Outer radius $b = 44.45$ mm
- Electrical conductivity $\sigma = 8.0 \times 10^6$ S/m
- Relative permeability (constant) $\mu_r = 200$

For these parameters, and an assumed impulsive exterior current, the FDTD calculation of the H-field and resulting E_z field was performed. Figure 2 presents the transient E-field at the $r = a$ which is the surface of the inner conductor, from this calculation.

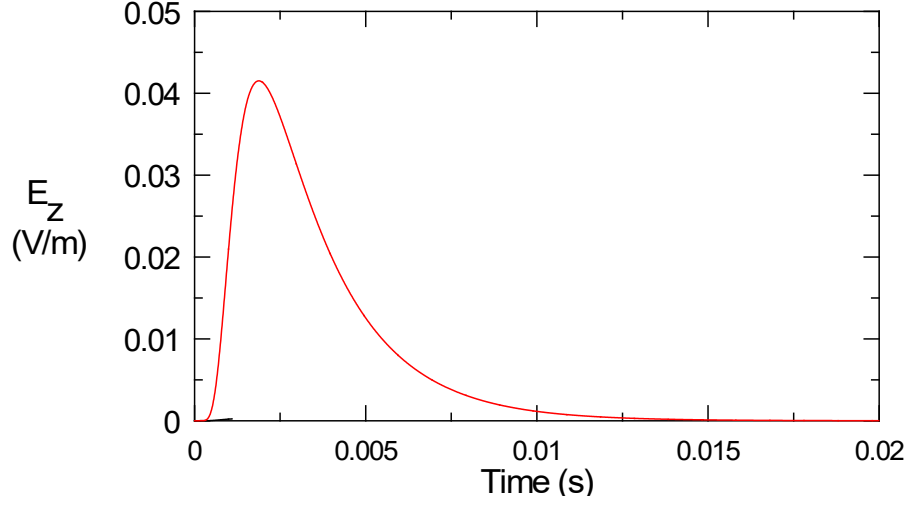


Figure 2. Plot of the transient E_z field at $r = a$ surface computed for the iron tube (constant $\mu_r = 200$) using the FDTD approach.

While this waveform appears reasonable, it is useful to compare its spectrum with that computed for the same conduit using the conventional frequency domain transfer impedance formula. As described in ref.[11], the transfer impedance for a single shield with diameter d , and thickness $\Delta = (b-a)$, is defined as

$$Z'_t(\omega) = R'_{dc} \frac{(1+j)\Delta/\delta}{\sinh((1+j)\Delta/\delta)} \quad (\Omega/\text{m}) \quad (16)$$

where R'_{dc} is the static per-unit-length resistance of the shield,

$$R'_{dc} = \frac{1}{\pi \sigma d \Delta} \quad (\Omega/\text{m}) \quad (17)$$

and δ is the electrical skin depth in the material, expressed as

$$\delta = \sqrt{\frac{2}{\omega \sigma \mu_r \mu_o}} \quad (\text{m}). \quad (18)$$

The term $\omega = 2\pi f$ is the angular frequency, σ is the conductivity, and the quantity $\mu_r \mu_o$ is the shield magnetic permeability, which is assumed to be a constant in this case.

Figure 3 presents a comparison of the transfer impedance of the iron conduit as calculated in the frequency domain using Eq. (16) (the dotted line). The result obtained from a Fourier transform of the FDTD solution is also shown in the figure. The process for this comparison is as follows: The time domain interior field is Fourier transformed to get $E_z(\omega)$, The unit impulse shield current is also Fourier transformed noting that the Fourier transform of an impulse is a constant. The frequency domain transfer impedance function is then obtained by dividing the interior field by the shield current in frequency domain. This is the

transfer impedance in frequency domain. As can be seen, the agreement between the two is excellent in Figure 3 indicating that the problem formulation and the numerical algorithm are correct.

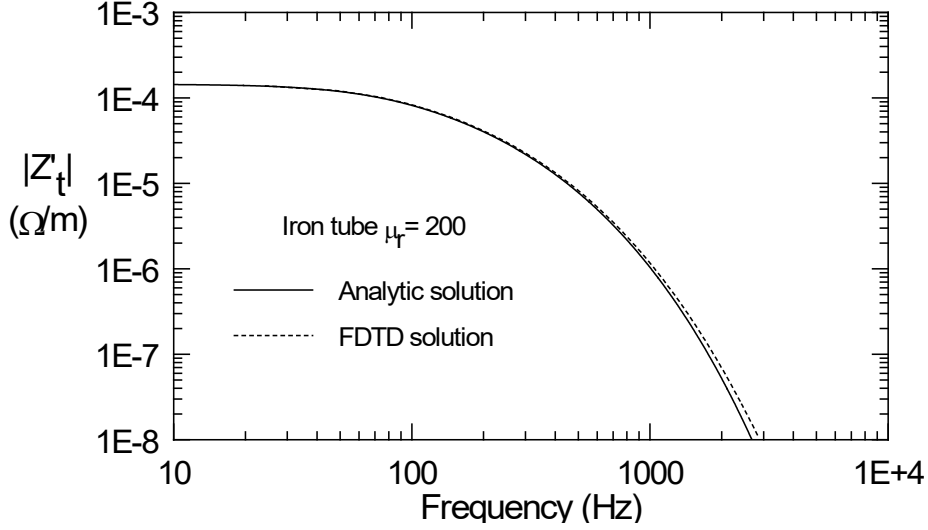


Figure 3. Comparison of the magnitude of the transfer impedance of the iron conduit, as calculated by the analytical expression and by the FDTD method.

3. Representation of the Nonlinear Permeability

In using the FDTD solution of Eq. (14) for a general ferromagnetic material, it is necessary to have a suitable way of describing the B-H curve of the material. As can be noted from Figure 4, there can be a very wide variation of the magnetization curves for different materials [12]. Using these curves, the value of $\mu(H)$ that is needed in Eq.(14) is the slope of the curve at a given value of H.

To provide a concrete example of this process, consider the B-H curve shown in Figure 5 for a Mn-Zn ferrite, as taken from ref.[13]. One suggested form for the slope of the B-H curve, and hence an approximation for $\mu(H)$, is given in [6] as

$$\mu(H) = \mu_o \left(1 + \frac{\mu_{ro} - 1}{1 + e^{\alpha(H-H_c)}} \right) \quad (19)$$

where $\mu_{ro} \approx$ the value of $\mu(0)$, and the parameters α and H_c control the shape of the magnetization curve. Recognizing this as the slope of the B-H curve, i.e., $dB/dH = \mu(H)$, this expression can be integrated analytically to provide the following B-H relationship:

$$B(H) = \mu_o \left[\mu_{ro} H + \frac{(\mu_{ro} - 1)}{\alpha} \ln \left(\frac{1 + e^{-\alpha H_c}}{1 + e^{-\alpha(H_c - H)}} \right) \right]. \quad (20)$$

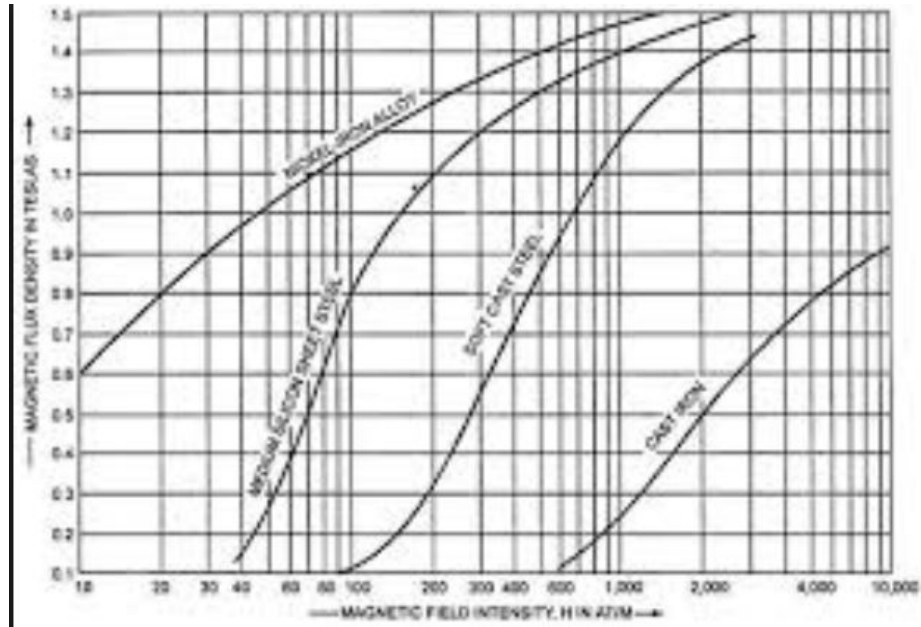


Figure 4. Illustration of the B-H magnetization curves for different materials. (Note that 1 oersted = 79.58 A/m and 1 gauss = 10^{-4} Tesla).

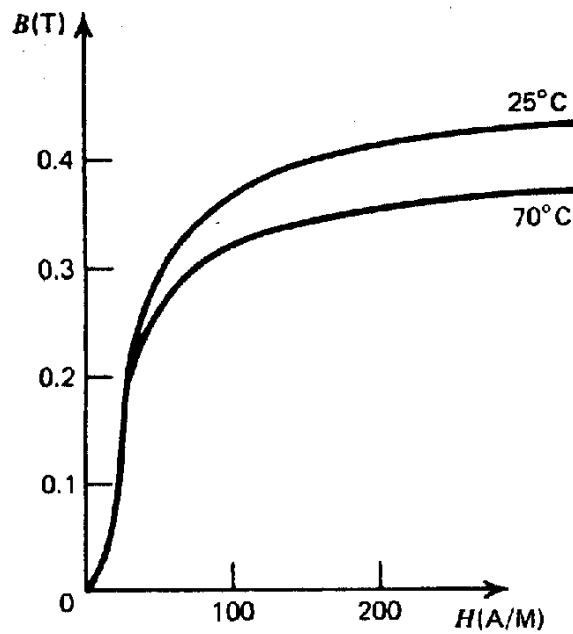


Figure 5. Plot of the magnetization curve for a Mn-Zn ferrite (taken from ref.[13]).

For the magnetization curve in Figure 5 for the 70°C case, the following parameters provide a reasonable fit to the magnetization data.

- $\alpha = 0.1$ (1/Tesla)
- $H_c = 45$ Tesla
- $\mu_{ro} = 6000$

Figure 6 plots the approximate magnetization curve obtained from Eq.(20) for this material. While it is not a perfect reproduction of Figure 5, it does provide a reasonable approximation. Given different magnetic materials, other parameters can be used in Eq.(19) to obtain a simple approximation for the material permeability for use in Eq.(14).

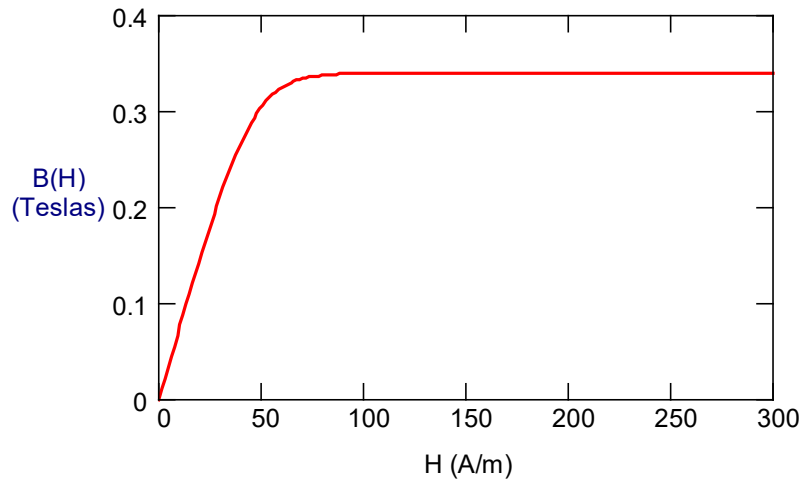


Figure 6. Plot of the curve-fit representation of the magnetization curve of Figure 5.

4. Computed Nonlinear Cable Response

Using the nonlinear diffusion model for the H-field, a sample calculation for the transient induced voltage within the iron conduit has been made. Unfortunately, detailed information about the behavior of the nonlinear material of this specific iron tube is not available, so certain assumptions have been made to illustrate the calculations. For this example, the hypothetical B-H magnetization curve of Figure 7 is assumed. This curve is selected to have an initial slope equal to $\mu = 170 \mu_0$, which corresponds roughly to the linear permeability of $\mu_r = 200$ used for the calculations in ref.[1]. The slope of this magnetization curve (relative to μ_0) is shown in Figure 8.

To generate the data in these figures, the following parameters for the magnetic material have been selected:

- $\alpha = 0.05$ (1/Tesla)
- $H_c = 50$ Tesla
- $\mu_{r0} = 200$

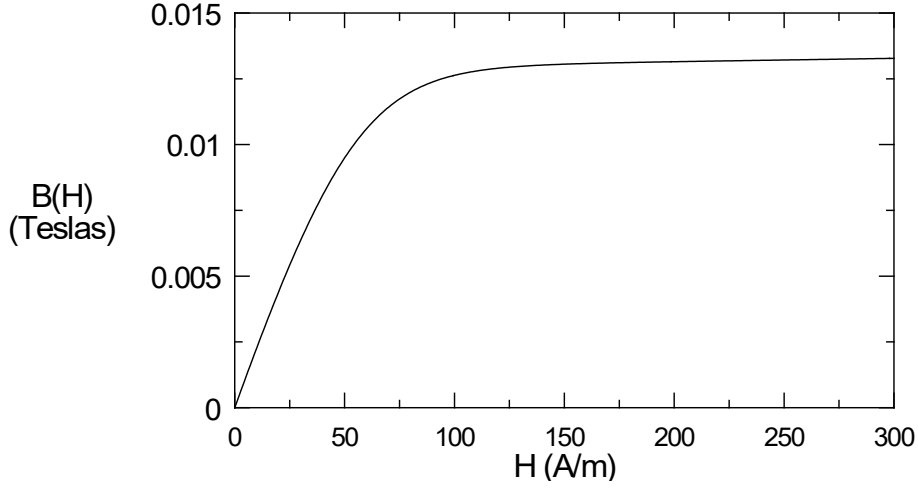


Figure 7. Assumed nonlinear magnetization curve for the iron conduit.

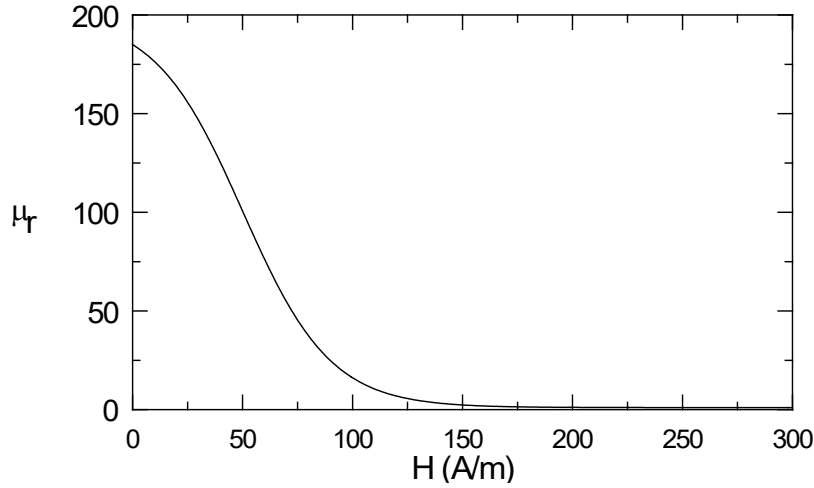


Figure 8. Nonlinear relative permeability μ_r from the magnetization curve of the iron conduit in Figure 7.

For the unit impulsive external shield current, Figure 9 plots the internal transient E_z field for the iron conduit resulting from the FDTD calculation of the H-field in the shield material. It is interesting to compare this waveform with that of the constant $\mu_r = 200$ case shown in Figure 2; the waveshapes in both cases are almost identical, but the amplitude of the nonlinear case is about 200 times smaller than for the linear material.

This seemingly strange behavior can be explained by examining Eq.(5), which may be re-written as

$$\frac{\partial H_\phi}{\partial t} = \frac{1}{\sigma \mu(H)} \left[\frac{1}{r} \frac{\partial}{\partial r} \left(r \frac{\partial H_\phi}{\partial r} \right) - \frac{H_\phi}{r^2} \right]. \quad (21)$$

For field points near the $r = b$ excitation surface of the conduit, the magnetic field strength is very large, and consequently, if the material is nonlinear, the value of μ_r is close to unity, which is the flat part of the B-H curve. In Eq. (3), $\mu(H)$ is 1 for the non-linear case and it is 200 for the linear case. This implies that the value of $\partial H / \partial t$ is about 200 times larger than

for the case of the linear material having $\mu_r = 200$. The fact that this time derivative (dH/dt) is larger in the nonlinear case by a factor of 200, implies that the local fields on or near the outside surface ($r = b$) of the conduit tend to decrease more rapidly in time than do those inside where the permeability remains high.

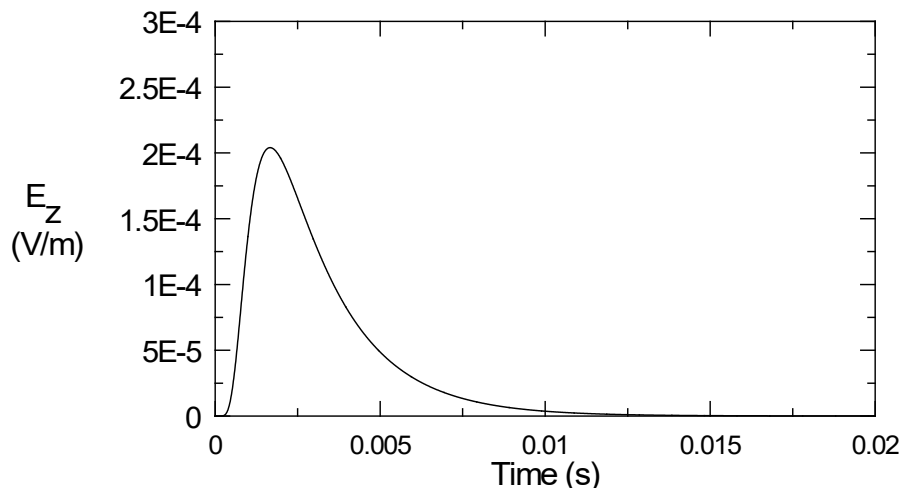


Figure 9. Plot of the transient internal E_z field for the case of the nonlinear iron conduit.

Deep inside the material, (say at $r = b - (\Delta/2)$) where the H-fields have decayed away to small values, the H-field strength is sufficiently low so that the permeability is back to its value of 200. This suggests that as the H-field continued to diffuse through the remainder of the conduit, and the interior E-field takes on the characteristic form of Figure 2, regardless of the saturation occurring at other locations. However, its amplitude is different, due to the reduction of the amplitude.

5. Discussion

This note has discussed an electrical model for estimating the effects of magnetic field saturation in a ferromagnetic conduit. Starting with Maxwell's equations, a suitable diffusion equation for the magnetic field within the conduit material due to an impressed current is developed. While this diffusion equation cannot be solved analytically, it can be solved numerically using a FDTD solution. The steps in performing this analysis are described, and several sample results are illustrated.

A key feature of this solution is the representation of the B-H magnetization curve of the conduit material by a suitable functional form. This is required for determining the dynamic permeability of the material, which is used as the calculation proceeds in time. Developing this curve requires detailed information about the magnetic behavior of the material, and in the sample case of the iron tube discussed here, these data are not available. As a result, the transient per-unit-length voltage source in Figure 9 resulting from the sample calculation is only an indication of what the actual result may be for the physical iron conduit.

Additional measurements of the magnetic properties of the iron tube are needed to better calculate understand the effects of saturation on the internal cable responses.

6. References

1. Tesche, F.M., "Direct-Strike Lightning Response Estimates of Buried Cables within a Communications Facility", Report prepared for Defense Procurement Agency, NEMP Laboratory, Spiez, Switzerland, November 11, 1997. Copy can be obtained from the second author DVG.
2. Tesche, F.M., "Stochastic Modeling of Direct-Strike Lightning Responses", Report prepared for Defense Procurement Agency, NEMP Laboratory, Spiez, Switzerland, November 30, 1997. Copy can be obtained from the second author DVG.
3. Young, F. J., "Ferromagnetic Shielding Related to the Physical Properties of Iron", *Proceedings of the 1968 IEEE International Symposium on EMC*, 1968, pp. 88-95.
4. Merewether, D. E., "EMP Transmission Through a Thin Sheet of Saturable Ferromagnetic Cable Shields", *IEEE Trans. EMC*, vol. EMC-11, pp. 139-143, Nov. 1969.
5. Merewether, D. E., "Analysis of the Shielding Characteristics of Saturable Ferromagnetic Material of Infinite Surface Area", *IEEE Trans. EMC*, vol. EMC-12, pp. 133-137, Aug. 1970.
6. Karzas, W. J., and T. C. Mo, "Linear and Nonlinear EMP Diffusion Through a Ferromagnetic Conducting Slab", *IEEE Trans. EMC*, vol. EMC-20, pp. 118-128, Feb. 1978.
7. Croisant, W. J, et. al., "A Nonlinear Analytical Procedure for Electromagnetic Transients in Ferromagnetic Shields", *Proceedings of the 1994 IEEE International Symposium on EMC*, Symposium Record 94CH3347-2, August 1994, pp. 190-195.
8. Croisant, W. J, et. al., "A Nonlinear Analytical Procedure for Electromagnetic Transients in Ferromagnetic Shields with an Exponential Permeability Model", *Proceedings of the 1995 IEEE International Symposium on EMC*, August 1995, pp. 614-619.
9. Lee, K. S. H., ed., **EMP Interaction: Principles, Techniques and Reference Data**, Hemisphere Publishing Co. New York, 1989.
10. Humphries, S., Jr., **Field Solutions on Computers**, CRC Press, Boca Raton, FL, 1997.
11. Tesche, F. M., et. al., **EMC Analysis Methods and Computational Models**, John Wiley and Sons, New York, December 1996.
12. Fink, D. G., and D. Christiansen, **Electronics Engineers' Handbook**, McGraw-Hill, New York, 1982.
13. Watson, J. K., **Applications of Magnetism**, John Wiley and Sons, New York, 1980.